Published in final edited form as:
Sci Signal. ; 5(209): ra9. doi:10.1126/scisignal.2002435.

PAS Kinase Promotes Cell Survival and Growth Through Activation of Rho1

Caleb M. Cardon[1], **Thomas Beck**[1,2,*], **Michael N. Hall**[2], and **Jared Rutter**[1,†]

[1]Department of Biochemistry, University of Utah School of Medicine, Salt Lake City, UT 84112, USA [2]Department of Biochemistry, Biozentrum, University of Basel, CH-4046 Basel, Switzerland

Abstract

In *Saccharomyces cerevisiae*, phosphorylation of Ugp1 by either of the yeast PASK family protein kinases (yPASK), Psk1 or Psk2, directs this metabolic enzyme to deliver glucose to the periphery for synthesis of the cell wall. However, we isolated *PSK1* and *PSK2* in a high-copy suppressor screen of a temperature-sensitive mutant of target of rapamycin 2 (*TOR2*). Posttranslational activation of yPASK, either by cell integrity stress or by growth on nonfermentative carbon sources, also suppressed the growth defect resulting from *tor2* mutation. Although suppression of the *tor2* mutant growth phenotype by activation of the kinase activity of yPASK required phosphorylation of the metabolic enzyme Ugp1 on serine 11, this resulted in the formation of a complex that induced Rho1 activation, rather than required the glucose partitioning function of Ugp1. In addition to phosphorylated Ugp1, this complex contained Rom2, a Rho1 guanine nucleotide exchange factor, and Ssd1, an mRNA-binding protein. Activation of yPASK-dependent Ugp1 phosphorylation, therefore, enables two processes that are required for cell growth and stress resistance: synthesis of the cell wall through partitioning glucose to the periphery and the formation of the signaling complex with Rom2 and Ssd1 to promote Rho1-dependent polarized cell growth. This complex may integrate metabolic and signaling responses required for cell growth and survival in suboptimal conditions.

INTRODUCTION

Organisms must monitor their environment to respond appropriately to changes in nutrient supply, temperature, and toxins. A critical decision made by organisms is whether to stimulate or arrest growth given the current environmental situation. In multicellular organisms, this decision depends on multiple signals, such as inputs from neighboring cells, hormonal cues, and neuronal signaling. In this context, making the wrong growth decision at a cellular level can lead to pathological consequences, including cancer. Cells from

†To whom correspondence should be addressed: rutter@biochem.utah.edu.
*Present address: Nestlé (Nestec Ltd.), Avenue Reller 22, 1800 Vevey, Switzerland.

Author contributions: C.M.C. performed all of the experiments. C.M.C. and J.R. designed the experiments and wrote the paper. T.B. and M.N.H. provided unpublished data that contributed to the initiation of this project.

Competing interests: J.R. is a consultant and Scientific Advisory Board member of BioEnergenix, LLC.

SUPPLEMENTARY MATERIALS
www.sciencesignaling.org/cgi/content/full/5/209/ra9/DC1
Fig. S1. Sorbitol (1 M) can suppress the *tor2*^{ts} growth phenotype.
Fig. S2. Ssd1-8A, but not Ssd1-8D or Ssd1-8E, overexpression is lethal in the JK9 strain.
Fig. S3. Neither *ROM1* nor *TUS1* is required for yPASK to suppress the *tor2*^{ts} growth phenotype.
Fig. S4. Rom2 and Ugp1 associate at both the permissive and the restrictive temperatures.
Fig. S5. Stability of Rom2 and Ssd1, but not Ugp1, decrease with extended heat shock.
Table S1. Strains and plasmids used.

multicellular organisms also have autonomous mechanisms to measure nutrient availability, which, when integrated with extrinsic signals, enables appropriate growth decisions.

Two evolutionarily conserved kinases that participate in this sensing and response are the 5′-adenosine monophosphate (AMP)–activated protein kinase (AMPK) (1) and the target of rapamycin (TOR) (2, 3). AMPK is activated when intracellular energy in the form of adenosine 5′-triphosphate (ATP) is depleted and promotes a switch from ATP consumption to ATP production (4). One primary aspect of this switch is a cessation of cell growth and division. The kinase activity of TOR is activated under nutrient-replete conditions and leads to an increase in protein translation and cell growth (2, 5). Hence, it has been called a master regulator of cell and organismal size in most organisms.

The *Saccharomyces cerevisiae* genome contains two closely related TOR-encoding genes, *TOR1* and *TOR2*. The protein products of these two genes function in two distinct protein complexes termed TOR complex 1 (TORC1) and TOR complex 2 (TORC2) (6–8). TORC1, which contains either Tor1 or Tor2, as well as Kog1, Tco89, and Lst8, regulates protein synthesis and cell size in response to nutrient availability. TORC1 function is inhibited by rapamycin. TORC2, which contains Tor2 (but not Tor1), Avo1, Avo2, Avo3, Bit61, and Lst8, is essential for cell division and cell cycle–dependent polarization of the actin cytoskeleton (9–11). TORC2 function is not directly sensitive to rapamycin. TORC2 regulates polarized cell growth at least partially through activation of the small guanosine triphosphatase (GTPase) Rho1 (12). To promote cell growth and division, Rho1 stimulates many downstream signaling pathways including protein kinase C (Pkc1)–mediated activation of mitogen-activated protein kinase (MAPK) signaling, activation of cell wall synthesis through the glucan synthase Fks1, and polarization of the actin cytoskeleton (13–16). Strains harboring a temperature-sensitive allele of *TOR2* (*tor2*^{ts}) arrest growth at the restrictive temperature (37°C) due to lack of TORC2 activity and decreased activation of Rho1 (6). This growth arrest can be suppressed by overexpression of proteins that activate Rho1. The growth arrest of the *tor2*^{ts} is also suppressed by growth on some nonfermentative carbon sources (carbon sources that are fermentable but do not cause glucose repression, such as raffinose) but not by nonfermentable carbon sources (glycerol, ethanol). Unexpectedly, treatment with agents that perturb the cell wall or cell membrane, which cause cell integrity stress, can also abrogate the *tor2*^{ts} phenotype (17). The mechanism underlying the connection between nonfermentative carbon sources or cell wall stress and suppression of the *tor2*^{ts} remains unresolved. These data suggest the presence of signaling modalities that control cell growth by integrating signals related to cell integrity and nutrient availability.

Many advances have occurred in our understanding of the inputs that are recognized by cell-autonomous nutrient sensors and of the nutrient sensors. The PAS kinase (PASK) family of kinases is required for normal energy balance in organisms from *S. cerevisiae* to mice (18, 19); however, the mechanisms whereby PASK signaling is integrated into broader cellular signaling networks have remained undiscovered. The *S. cerevisiae* genome contains two closely related and partially redundant PASK paralogs, *PSK1* and *PSK2* (referred to together as yPASK). In yeast, the activity of yPASK is stimulated by the WSC family of cell membrane sensors in response to stresses that compromise cellular integrity (20). Cellular nutrient status can also activate yPASK through an interaction with the AMPK (known in yeast as Snf1) signaling pathway. Both Psk1 and Psk2 phosphorylate Ser^{11} of Ugp1, the enzyme responsible for the synthesis of uridine 5′-diphosphate glucose (UDP-glucose), which is the glucose donor for glycogen and cell wall glucan production. Surprisingly, phosphorylation at Ser^{11} does not affect the enzymatic activity of Ugp1, but rather influences the destination of the glucose moiety from UDP-glucose (21). In the unphosphorylated state, Ugp1 synthesizes UDP-glucose that is used preferentially for the

synthesis of glycogen. In the phosphorylated state, Ugp1 produces UDP-glucose that is partitioned preferentially toward production of cell wall glucans. Therefore, a yPASK-null strain (*psk1*Δ *psk2*Δ) exhibits a marked increase in glycogen content at the expense of cell wall glucan, indicating an inability to properly regulate glucose flux (21). All yPASK mutant phenotypes are completely phenocopied by mutating Ugp1 Ser^{11} to alanine (Ugp1-S11A), which prevents Ugp1 phosphorylation (21). Thus, the effects of yPASK on glucose partitioning are primarily mediated through Ugp1 phosphorylation.

In a screen for multicopy suppressors of the lethality of a *tor2*^{ts} mutant, we discovered both *PSK1* and *PSK2*. We found that the signaling mechanism by which yPASK suppresses the *tor2*^{ts} requires phosphorylation of Ugp1. We show that phosphorylated Ugp1 enables the formation of a signaling complex, containing phosphorylated Ugp1, the mRNA-binding protein Ssd1, and the Rho guanine nucleotide exchange factor (RhoGEF) Rom2, which leads to the activation of Rho1. The activation of Rho1, in response to yPASK-dependent phosphorylation of Ugp1, stimulates cell survival and division. Thus, yPASK coordinates cell growth through its effects on glucose partitioning and Rho1.

RESULTS

yPASK activity is both necessary and sufficient to suppress the *tor2*^{ts} growth phenotype

As a component of TORC2, Tor2 is essential for viability (6). Because a *tor2*Δ deletion mutant is inviable, we used a temperature-sensitive *tor2*^{ts} mutant to conduct a high-copy suppressor screen for previously unknown genes that bypass the essential role of Tor2 in cell survival and growth. This screen should reveal genes that encode proteins that function downstream of Tor2 or genes that encode proteins activating similar growth pathways independently of Tor2. We recovered genomic fragments that contained *RHO2*, *PSK1*, and *PSK2*, all of which suppressed the growth defect of the *tor2*^{ts} strain at the restrictive temperature (Fig. 1A). Overexpression of *RHO2* likely suppressed the *tor2*^{ts} by functioning in a manner analogous to that of *RHO1* (12), given the structural and functional similarities between Rho1 and Rho2. Overexpression of either *PSK1* or *PSK2* from their endogenous promoters supported growth of the *tor2*^{ts} at the restrictive temperature, confirming the results of the high-copy suppressor screen. This suppression required kinase activity, because a *PSK2* kinase domain mutant (K870R) failed to restore growth of the *tor2*^{ts} mutant, and overexpression of the kinase domain alone suppressed the *tor2*^{ts} growth phenotype (Fig. 1B).

Given that all of the known *psk1*Δ *psk2*Δ phenotypes are completely phenocopied by the *UGP1-S11A* allele (21), we tested whether Ugp1 phosphorylation was necessary for suppression. In the presence of the un-phosphorylatable Ugp1-S11A protein, neither *PSK1* nor *PSK2* enabled growth of the *tor2*^{ts} mutant, showing that Ugp1 phosphorylation is necessary for yPASK-dependent suppression (Fig. 1C). Because S11E and S11D mutants of Ugp1 do not mimic the phosphorylated state, but rather mimic the constitutively unphosphorylated state (21), we were unable to determine whether Ugp1 phosphorylation is sufficient for *tor2*^{ts} suppression.

yPASK activation suppresses the *tor2*^{ts} and increases Ugp1 phosphorylation

The *tor2*^{ts} mutant is unable to grow at high temperature (37°C) presumably because of decreased functional TORC2. Growth of the *tor2*^{ts} mutant can be rescued by supplementation with the osmotic stabilizer sorbitol (6), suggesting that one of the lethal defects in this mutant is instability of the cell wall. We reproduced the suppression of the *tor2*^{ts} growth phenotype by supplementation of 1 M sorbitol in the medium (fig. S1) However, treatment with agents that destabilize the cell membrane or cell wall (for example,

calcofluor white, congo red, SDS, or Tween) suppresses rather than exacerbates the *tor2*^{ts} mutant phenotype (17). The mechanism by which cell integrity stress suppresses the *tor2*^{ts} is unknown, but we speculated that yPASK might be involved because it is activated by cell integrity stress (20) and suppresses the *tor2*^{ts} when overexpressed. Therefore, we tested the necessity of yPASK for suppression of the *tor2*^{ts} by cell integrity stress. Because Psk2 responds more robustly to cell integrity stress than does Psk1 (20) and because *PSK2* overexpression more fully suppressed the *tor2*^{ts} when compared to *PSK1*, we focused primarily on the role of *PSK2*. Addition of 0.005% SDS to the medium suppressed the *tor2*^{ts} phenotype (Fig. 2A); however, the *tor2*^{ts} strain also containing the *psk2*Δ mutation failed to grow on the SDS-supplemented medium (Fig. 2A). Consistent with the known role of Psk2 in cell integrity stress response, the *psk2*Δ mutant showed a modest growth defect on SDS-supplemented medium (Fig. 2A, top right). Suppression of the *tor2*^{ts} phenotype in response to cell integrity stress depended on phosphorylation of Ugp1 at Ser^{11} (Fig. 2A). Therefore, in the presence of normal Tor2 signaling, Psk2 and the phosphorylation of Ugp1 are not required for viability during cell integrity stress, but become essential upon Tor2 inactivation. Thus, activation of yPASK through two independent mechanisms, cell integrity stress or overexpression, bypassed the *tor2*^{ts} mutant phenotype.

In addition to cell integrity stress, growth on nonfermentative carbon sources also activates yPASK (20). Growth on either raffinose or galactose, which are nonfermentative carbon sources that activate yPASK, suppressed the *tor2*^{ts} phenotype (Fig. 2B). Deletion of *PSK2* or the presence of Ugp1-S11A, however, attenuated the suppression of the *tor2*^{ts} phenotype by the nonfermentative carbon sources. Together, three independent means of enhancing yPASK signaling—overexpression of *PSK1* or *PSK2*, cell integrity stress, or growth on nonfermentative carbon sources—all suppressed the *tor2*^{ts} phenotype in a manner dependent on Ugp1 Ser^{11}.

To confirm that these suppressing conditions increased Ugp1 phosphorylation, we performed immunoblots with an antibody specific for phospho–Ser^{11}-Ugp1 (Fig. 2C). A small amount of phosphorylated Ugp1 was detected under basal conditions, but the conditions that should stimulate yPASK activity increased Ugp1 phosphorylation. Thus, activation of yPASK was sufficient to suppress the *tor2*^{ts} growth phenotype, and that suppression required Ugp1 phosphorylation.

SSD1 is required for the *tor2*^{ts} suppression by yPASK

The studies described so far were conducted in the JK9 strain background. However, we found that yPASK failed to suppress the *tor2*^{ts} growth phenotype in the W303 strain background (Fig. 3A, right panel). We reasoned that determining the key difference between the JK9 and the W303 strains should provide insight into the genetic pathway underlying yPASK-dependent suppression. To uncover the genetic basis for this distinction, we took a candidate gene approach by examining known polymorphisms that vary between the two strains. Many laboratory *S. cerevisiae* strains have a mutation (*ssd1d*) that causes a premature stop codon in the *SSD1* gene (22). *SSD1* has been implicated genetically in many different cellular functions, but the biochemical function of Ssd1 has remained elusive (23–32). It has homology to the ribonuclease II (RNase II) family of enzymes, but it lacks residues that are critical for catalytic activity. Clues to Ssd1 biochemical function have come from studies showing that Ssd1 controls posttranscriptional gene expression through direct mRNA binding (24, 33).

The W303 strain contains the nonfunctional *ssd1d* allele, whereas the JK9 strain contains wild-type *SSD1* (25). To determine whether this mutation is the key difference preventing suppression of the *tor2*^{ts} by yPASK in the W303 strain, we complemented the *ssd1d* mutation with a plasmid containing the wild-type *SSD1* gene. When wild-type *SSD1* was

present, yPASK suppressed the *tor2*^{ts} phenotype in the W303 strain background (Fig. 3A). Conversely, deletion of the wild-type copy of *SSD1* in the JK9 strain prevented yPASK suppression of the *tor2*^{ts} growth defect. These data indicated that *SSD1* was necessary for yPASK to suppress the *tor2*^{ts} and was epistatic to yPASK.

The function of Ssd1 in posttranscriptional gene regulation is regulated by phosphorylation at eight N-terminal sites by the protein kinase Cbk1 (24). Six of these phosphorylation sites are a perfect match for the yPASK consensus phosphorylation motif (HXRXX[S/T]) (34). To determine whether Ssd1 phosphorylation at these sites might also play a role in yPASK-mediated suppression of the *tor2*^{ts} growth phenotype, we created mutants of Ssd1 wherein the eight phosphorylatable residues were mutated to alanine (Ssd1-8A) or a phosphomimetic amino acid (Ssd1-8D or Ssd1-8E). Overexpression of nonphosphorylatable Ssd1 was previously observed to cause toxicity (24), which was due to its role in gene expression. As expected, we also observed that overexpression of Ssd1-8A caused toxicity, which was not observed when wild-type Ssd1 or Ssd1 containing the phosphomimetic substitutions was overexpressed (fig. S2). All of these *SSD1* mutants, like the wild type, enabled suppression of the *tor2*^{ts} phenotype by *PSK2* (Fig. 3B), suggesting that phosphorylation of Ssd1 at these eight sites does not play an essential role in yPASK-dependent suppression of the *tor2*^{ts} phenotype. Thus, the role of Ssd1 in *tor2*^{ts} suppression is likely distinct from its role in posttranscriptional regulation of gene expression.

Ugp1 and Ssd1 physically interact in a phosphorylation-dependent manner

To investigate whether Ugp1 and Ssd1 physically interacted as part of their role in suppression of the *tor2*^{ts} growth phenotype, we expressed a C-terminally hemagglutinin (HA)–tagged Ssd1 at normal abundance (native promoter/CEN plasmid) and tested for a possible interaction with Ugp1. Because Ugp1 phosphorylation was critical in the *tor2*^{ts} strain at 37°C, we performed the coimmunoprecipitations at 37°C. Presumably, because Ugp1 is an abundant protein, control immunoprecipitations often showed trace amounts of Ugp1. However, we detected wild-type Ugp1 immunoprecipitated with Ssd1-HA above the background detected in the control samples (Fig. 3C). Unlike the wild-type, we detected no interaction of the S11A mutant of Ugp1 with Ssd1-HA (Fig. 3C).

Because of the various other cellular roles that both Ugp1 and Ssd1 play in growth and stress response, we examined whether this association was dynamically regulated in response to a temperature increase. In cultures grown at 37°C for 0, 3, and 5 hours, complex formation was initially enhanced in response to the temperature shift, but subsequently decreased after 5 hours at 37°C (Fig. 3C). Together, these data indicated that Ssd1 and Ugp1 formed a heat stress–responsive complex that was dependent on Ugp1 phosphorylation.

The *tor2*^{ts} suppression effect of Ugp1 phosphorylation is independent of effects on glucose partitioning

Because the osmotic stabilizer sorbitol rescues growth of the *tor2*^{ts} mutant and because phosphorylation of Ugp1 promotes increased cell wall glucan production, which increases cell wall stability (21), we investigated whether this function of Ugp1 was important for yPASK-dependent suppression of the *tor2*^{ts} mutant phenotype. This question cannot be answered directly because a catalytically inactive mutant of Ugp1 does not enable viability of a *ugp1*Δ strain, due to the essential role of Ugp1 in producing UDP-glucose (35). However, we conducted two experiments that suggested that the *tor2*^{ts} suppression role of Ugp1 was distinct from its role in glucose partitioning.

Overexpression of phosphoglucomutase-2 (*PGM2*) suppresses a growth defect caused by loss of Ugp1 phosphorylation (19). Pgm2 converts glucose-6-phosphate to glucose-1-

phosphate, which is the glucose donor for UDP-glucose synthesis by Ugp1. When it is overexpressed, the increased UDP-glucose synthesis enables cell wall production and stabilization, even in the absence of Ugp1 phosphorylation (36). If cell wall glucan synthesis was sufficient for *tor2*^{ts} suppression, *PGM2* overexpression might be expected to suppress the growth phenotype. However, *PGM2* overexpression had no effect on the temperature sensitivity of the *tor2*^{ts} mutant (Fig. 4A).

If Ugp1 phosphorylation regulates glucose partitioning and *tor2*^{ts} suppression through the same mechanism, then these two functions should both depend on *SSD1*. To determine whether yPASK-dependent regulation of glucose partitioning was dependent on *SSD1*, as we had found for *tor2*^{ts} suppression by *PSK2* overexpression (Fig. 3), we measured glycogen content in wild-type and *psk1*Δ *psk2*Δ mutants in both the JK9 and the W303 backgrounds both with and without *SSD1* (Fig. 4B). The *psk1*Δ *psk2*Δ mutant exhibited glycogen content that was markedly higher than that of wild type, consistent with our previous results (21). The fold increase in glycogen content in the *psk1*Δ *psk2*Δ mutant relative to wild type was not significantly different in either the JK9 or the W303 strain with or without functional *SSD1* (Fig. 4B). Although yPASK deletion caused an increase in glycogen content in each genetic condition, there was an overall decrease in glycogen content in the JK9 strain with *SSD1*, which we think is likely due to an interaction between *SSD1* and one or more genes other than *PSK1* or *PSK2*.

These data, together with the *PGM2* data, indicate that there is a bifurcation in the yPASK pathway at the point of Ugp1 phosphorylation. Suppression of the *tor2*^{ts} through phosphorylation of Ugp1 requires Ssd1. However, the ability of Ugp1 phosphorylation to enact the switch from production of UDP-glucose for glycogen to use in cell wall glucans is independent of Ssd1. These data would indicate that Ssd1 is not required for Ugp1 phosphorylation but may be necessary downstream of phosphorylation for the signaling function of Ugp1 that allows cells to tolerate loss of Tor2 function. Consistent with the hypothesis that Ssd1 is downstream of Ugp1 phosphorylation, yPASK-dependent phosphorylation of Ugp1 increased in response to heat shock in the absence of Ssd1 (Fig. 4C). However, the *ssd1*Δ mutant consistently had less total phospho-Ugp1. These data indicate that Ssd1 is not required for Ugp1 phosphorylation in response to yPASK activation, but it may be required to fully stabilize the phosphorylated form.

yPASK promotes Rom2-dependent Rho1 activation

Tor2 mediates most of its effects on cell growth and actin reorganization through activation of the small GTPase Rho1 (37). Rho1 controls activation of the MAPK pathway, cortical actin polarization, cell wall synthesis, and budding (14–16). Because of the critical role of Rho1 in mediating the effects of Tor2 activation on growth, we postulated that the ability of yPASK to suppress the *tor2*^{ts} might also be dependent on Rho1 activation, which is usually caused by GEFs. The *S. cerevisiae* genome encodes three GEFs for Rho1, *ROM1*, *ROM2*, and *TUS1* (38, 39). To determine whether Rho1 activation by one of these GEFs was required for suppression of the *tor2*^{ts} by yPASK, we examined suppression in strains each lacking one GEF. Whereas deletion of *ROM1* or *TUS1* had no effect on yPASK-dependent *tor2*^{ts} suppression (fig. S3), it was completely abolished by deletion of *ROM2* (Fig. 5A). Because Rom2, like Ssd1, was required for suppression and Ssd1 was present in a complex with Ugp1, we investigated whether Rom2 was also a component of this complex. A FLAG-tagged Rom2 protein expressed from the endogenous *ROM2* locus precipitated wild-type Ugp1, and this interaction depended on Ugp1 Ser^{11} (Fig. 5B). At both the permissive and the restrictive temperatures, Rom2 and Ugp1 were physically associated (fig. S4). We noted a substantial decrease in Rom2 protein after 3 hours at 37°C (fig. S5). The instability of

Rom2 at the restrictive temperature makes it difficult to quantitatively evaluate changes in the Rom2-Ugp1 association.

Because we found that the Ssd1-Ugp1 interaction was dynamic in response to high temperature, we examined the kinetics of the Rom2-Ugp1 interaction. The kinetics of the association between Rom2 and Ugp1 were similar to those of Ssd1 and Ugp1. The degree of association was greatest in cells incubated for 3 hours at 37°C, and the interaction returned close to baseline by 5 hours (Fig. 5C). To more systematically assess protein abundance, we grew cultures at 37°C and harvested samples every hour for 7 hours. By Western blotting, we observed an apparent decrease in the abundance of Rom2 and Ssd1 after about 4 hours at 37°C (fig. S5), whereas Ugp1 appeared stable over the course of the heat shock treatment. Ugp1 phosphorylation appeared to peak after 1 to 2 hours at 37°C and then gradually decreased over the remainder of the time course.

Ugp1 could form either two distinct complexes, one with Rom2 and another with Ssd1, or a single complex with both Ssd1 and Rom2. Tagged forms of Ssd1 and Rom2 coimmunoprecipitated from yeast grown at 37°C (Fig. 5D) and Ssd1 and Ugp1 failed to interact in a *rom2*Δ strain (Fig. 5E), suggesting that the pairwise interactions are stabilized in the context of the entire complex. Because yPASK suppression of the $tor2^{ts}$ growth phenotype required *ROM2* and Rom2 interacted with Ssd1 and phospho-Ugp1, we speculated that this Rom2 complex promotes Rho1 activation and thereby bypasses the requirement for Tor2 activity. Therefore, we determined whether *PSK2* overexpression was sufficient to activate Rho1 in the $tor2^{ts}$ mutant strain by monitoring the amount of guanosine 5′-triphosphate (GTP)–bound (active) Rho1 isolated with Rho1 binding domain (RBD)–conjugated beads by Western blotting (40, 41). The $tor2^{ts}$ strain at the nonpermissive temperature had an attenuated amount of active Rho1 when compared to wild-type cells (Fig. 5F). Overexpression of *PSK2* in the $tor2^{ts}$ mutant, however, increased the amount of GTP-bound Rho1 to slightly above that of wild type. Thus, we concluded that yPASK overexpression caused Ugp1 phosphorylation, the formation of a Ugp1-Ssd1-Rom2 complex, and the activation of Rho1, which suppressed the growth defect of the $tor2^{ts}$ mutant.

DISCUSSION

Activation of yPASK, through overexpression, cell integrity stress, or growth on non-fermentative carbon sources, increased Ugp1 phosphorylation and suppressed the $tor2^{ts}$ growth phenotype. Ugp1 phosphorylation nucleated the formation of a signaling complex that contained a metabolic enzyme (Ugp1), a degenerate RNase (Ssd1), a Rho1 GEF (Rom2), and possibly other proteins. The roles of Ugp1 and Ssd1 within this complex appear to be separable from their defined roles in glucose utilization (20, 21) and translational repression (24, 33), respectively. We found that this complex appears to activate Rho1, thereby functioning in cellular growth control. Although in many of our experiments, Psk2 was more effective in suppressing the growth defect of $tor2^{ts}$, we believe that this is likely due to differences in protein abundance rather than a difference in function between Psk1 and Psk2, which is consistent with their functional redundancy in regulating glucose partitioning (20).

Within the Ugp1, Ssd1, Rom2 complex, it is most likely that Rom2 mediates Rho1 activation, because Rom2 has Rho1 GEF activity (17). Rho1 has at least four downstream effectors. It binds to and activates Pkc1 (37), which activates the MAPK signaling cascade. Rho1 activates cell wall synthesis by binding to and activating the β-1,3-glucan synthase Fks1 (15). Finally, Rho1 interacts with Bni1, a formin family member (16), and Skn7, a two-component signaling factor (42). However, activation of Rho1 does not always produce

equivalent activation of all of the downstream effectors; Rho1 activation can preferentially activate specific downstream effectors, which is at least partially dependent on the activating GEF. We found that yPASK-dependent suppression of the *tor2*^{ts} appeared to function exclusively through Rom2, and not Rom1 or Tus1, two other verified Rho1 GEFs, and this may be because only Rom2 assembles in the Ugp1-Ssd1 complex. The *tor2*^{ts} strain exhibits growth arrest with a disorganized actin cytoskeleton (37), which can be suppressed by overexpression of Pkc1. However, overexpression of the other Rho1 downstream effectors, Bni1, Fks1, or Skn7, does not suppress the *tor2*^{ts} growth phenotype (37). These data, and the fact that growth on sorbitol suppresses the *tor2*^{ts}, indicate that the lethal defects of the *tor2*^{ts} strain are lack of actin organization and cell lysis probably due to cell wall defects. Given that yPASK activation can suppress the *tor2*^{ts}, yPASK signaling most likely repairs one or both of these defects through the activation of Rho1. This could be accomplished by Rho1-dependent activation of Pkc1 and actin rearrangement, activation of Fks1 and cell wall synthesis, or both. It remains to be determined which Rho1 downstream effectors are regulated by yPASK activation and which are required for *tor2*^{ts} suppression.

Ssd1 is required for yPASK to suppress the *tor2*^{ts} growth phenotype. The role of Ssd1 in this signaling pathway remains unclear. Its physical interaction with Ugp1 in a phosphorylation-dependent manner, however, strongly suggests that its suppressing function is as a component of the Ugp1-Rom2 complex. Two possible roles for Ssd1 in this complex are (i) to stabilize the phosphorylated form of Ugp1 or (ii) to function as a scaffold for the Rom2-Ugp1 association. The absence of Ssd1 decreased the amount of phosphorylated Ugp1, suggesting that Ssd1 may prevent Ugp1 dephosphorylation (Fig. 4C). This effect, however, could be a secondary effect of binding with Ssd1 and Rom2. The model of Ssd1 as a scaffold is particularly attractive, because it would bring together Ugp1, the recipient of the activating phosphorylation signal, and Rom2, which likely provides the Rho1 activation output.

The RNA binding capacity of Ssd1 raises the intriguing possibility that the complex also contains RNA. The complex may function to regulate specific mRNA stability, localization, or translation, or, alternatively, RNA may play a structural or regulatory role within the complex. Unlike the described role of Ssd1 in translational repression (24), the function of Ssd1 in suppression of the *tor2*^{ts} was unaffected by phosphorylation on the known eight N-terminal residues. Phosphorylation of Ssd1 also promotes asymmetric mRNA localization, which may have a role in polarized cell growth (33). These data indicate that the two roles of Ssd1 are separable and likely represent distinct activities. One is regulated by phosphorylation at the N terminus and involves regulation of mRNA translation and localization. The other involves complex formation with Ugp1 and Rom2, which is independent of N-terminal phosphorylation. This duality may enable coordination between the cell wall synthesis and actin polarization required for cell division and the spatially regulated expression of cell wall–degrading enzymes that are needed for cell separation.

The primary mechanism by which yPASK regulates the Rho1-activating complex appears to be phosphorylation of Ugp1. Therefore, the phosphorylation of Ugp1 plays at least two cellular roles. First, it causes the preferential partitioning of UDP-glucose toward cell wall biosynthesis at the expense of glycogen storage (21). This function is independent of Ssd1. Second, Ugp1 phosphorylation nucleates the formation of a signaling complex that includes Ssd1 and Rom2. Although these two effects are separable on the basis of their differential Ssd1 dependence, they may be indirectly related. The yPASK-dependent translocation of Ugp1, which might be the mechanism of glucose partitioning, may also be required for the formation of the Ugp1-Ssd1-Rom2 complex. Peripheral localization would bring the complex into proximity with Rho1, which is known to localize to the cell periphery (43). The two functions of Ugp1 may both be dependent on translocation and may allow Ugp1 to

simultaneously produce UDP-glucose at the cell periphery and activate the Fks1 protein (through Rho1), which is responsible for the incorporation of UDP-glucose in cell wall biogenesis. Thus, Ugp1, thought only to catalyze the formation of UDP-glucose, has a distinct signaling function. It remains to be determined, however, whether this signaling function is dependent on the enzymatic activity of Ugp1 or Ugp1 simply plays a scaffolding role within the complex. If enzymatic activity is required, it would be interesting to determine the role of UDP-glucose in the complex. This is a difficult question to answer given that the enzymatic activity of Ugp1 is required for cell viability and that Ugp1 forms a stable octamer (35). However, future studies will ultimately shed light on the molecular basis of the signaling activity of this metabolic enzyme.

The physiological significance of yPASK activation remains to be elucidated. One possibility is that yPASK is simply activated in response to various forms of stress, both structural and metabolic, and acts to stabilize the cell wall. This is accomplished by phosphorylation of Ugp1, which directly promotes cell wall production, and also activates Rho1, which leads to an increase in cell wall biogenesis through activation of Fks1. On the other hand, yPASK activation might enable growth under nonideal conditions. Rho1 activation leads to polarization of the actin cytoskeleton in coordination with cell growth and division. A pro-growth role for yPASK is supported by the observation that an *fks1*Δ mutation suppresses the growth defect of $tor2^{ts}$ (6). If yPASK were suppressing the $tor2^{ts}$ by simple up-regulation of cell wall synthesis, deletion of *FKS1* should exacerbate and not suppress the $tor2^{ts}$ phenotype. This proposed pro-growth role is further supported by the fact that yPASK is a positive regulator of protein synthesis in yeast (19), which is clearly a pro-growth function. In mammalian systems, PASK is activated in nutrient-replete conditions to elicit the appropriate cellular response (18). Specifically, PASK promotes insulin synthesis in pancreatic β cells, represses oxidative metabolism in skeletal muscle, and up-regulates lipid synthesis and storage in the liver. These data support an evolutionarily conserved role for the PASK family in mediating nutrient-responsive anabolism.

Herein, we detailed a signaling network that connects PASK and TOR signaling. There are many similarities between PASK and TOR in *S. cerevisiae* and in mammals. First, TOR responds to nutrient-replete conditions, both locally and globally, to elicit a pro-growth response (6). This function is analogous to the roles described in this study and elsewhere for PASK. Second, PASK and TOR both have two closely related paralogs in *S. cerevisiae* (*PSK1*, *PSK2* and *TOR1*, *TOR2*), but higher organisms only have one of each gene. Third, mice lacking PASK and mice lacking S6 kinase 1 (S6K1), a downstream target of TOR signaling, have an overlapping set of phenotypes (18, 44). Specifically, they both exhibit increased metabolic rate, are resistant to diet-induced obesity, and have β cell insufficiency. These similarities could be coincidental, but it is also possible that these two highly conserved nutrient-sensing kinases have a closer relationship. Whereas we have shown that yPASK and TORC2 function in parallel pathways in *S. cerevisiae* to activate Rho1, their functions in higher organisms might be in more direct coordination.

The cell-autonomous decision to grow and divide must be responsive to environmental cues. In particular, it must integrate the nutritional environment to ensure that sufficient energy sources and building blocks are available. Because of the potential catastrophic consequences of mishandling this decision, cells have evolved multiple cellular energy sensors to detect the nutritional environment and signal appropriately. We have shown that yPASK functions in parallel to TORC2 to enable cell survival and growth under stress conditions.

MATERIALS AND METHODS

Yeast cells, culture media, and materials

S. cerevisiae strain JRY626 (MAT*a leu2 ura3 trp1 his4*) was used as the JK9 parental strain and wild-type strain. JRY421 (MAT*a*/α *his3 lys2 met15 ura3 trp1 leu2*) was used as the W303 parental diploid. Temperature-sensitive strains were isolated by sporulation and dissection. Deletion mutant strains and strains expressing chromosomal-integrated FLAG-tagged proteins were generated by standard polymerase chain reaction (PCR)–based homologous recombination methods in diploids, followed by sporulation and tetrad dissection (45). Yeast were transformed by the lithium acetate method and grown at 30°C in SD medium (0.67% yeast nitrogen base, 2% glucose) with amino acids unless otherwise indicated. Complete strain and plasmid information is given in table S1.

For the growth assays, strains of the indicated genotypes were grown to saturation and serially diluted in water. These diluted samples were spotted onto synthetic minimal medium lacking the appropriate amino acid for selection (uracil or uracil and methionine) and with the indicated additives and incubated at the indicated temperature for 3 to 4 days. Growth experiments were performed four to six times.

Glycogen determination

Glycogen assay was performed as previously described (19). Briefly, UDP-glucose pyrophosphorylase (UGPase) activity was determined by the rate of formation of glucose-1-phosphate from UDP-glucose in a nicotinamide adenine dinucleotide phosphate (NADP)–linked glucose-6-phosphate dehydrogenase assay as previously described (35). The reaction mixture contained 50 mM tris (pH 8.0), 10 mM dithiothreitol, 10 mM $MgCl_2$, 0.2 mM NADP, 10 mM glucose-1,6-biphosphate, 2 mM UDP-glucose, 0.6 U of phosphoglucomutase, 0.5 U of glucose-6-phosphate dehydrogenase, 10 mM sodium pyrophosphate, and sample (whole-cell lysate). Assay was read at 340 nm in a 1-cm path cuvette in an Ultrospec 2000 spectrophotometer (Amersham Pharmacia).

Immunoprecipitation

For Ugp1-Rom2 and Ugp1-Ssd1 coimmunoprecipitation experiments, the indicated strains were grown to log phase, harvested, resuspended, and lysed in 600 μl of immunoprecipitation (IP) buffer [25 mM potassium acetate (KOAc), 25 mM Hepes (pH 7.4), 0.2 mM EDTA, 0.2 mM EGTA, 10% glycerol, 0.02% NP-40, protease inhibitor cocktail (Sigma), and PhosSTOP (Roche)]. Cleared cell lysates were incubated with either anti-FLAG– or anti-HA–conjugated (Sigma) beads for 2 hours at 4°C. The mixture was then rinsed two times in IP buffer. The beads were re-suspended in IP buffer and transferred into a spin column (Sigma). The beads were rinsed three times in wash buffer [50 mM KOAc, 25 mM Hepes (pH 7.4), 0.2 mM EDTA, 0.2 mM EGTA, 10% glycerol, 0.02% NP-40, protease inhibitor cocktail, and PhosSTOP]. The beads were incubated with FLAG or HA peptide for 1 hour at room temperature and the elution was mixed with Laemmli's loading buffer. The samples were then analyzed by Western blot with the appropriate antibody [anti-FLAG (Cell Signaling), anti-HA (Covance), and P-Ugp1 (Cell Signaling)].

Pull-down assay for active Rho1

Active Rho1 was assayed as previously described with modification (40, 41). Rho1-HA–expressing cells were grown to log phase, harvested, and lysed in IP buffer [25 mM Hepes-KOH (pH 7.9), 100 mM KOAc, 0.2 mM EDTA, 0.2 mM EGTA, 0.1% NP-40, 10% glycerol, protease inhibitor cocktail (Sigma), and PhosSTOP (Roche)]. Cleared cell lysates were normalized with the Bradford assay. Normalized cell lysates were incubated with

glutathione *S*-transferase (GST)–tagged RBD preconjugated to beads (Cytoskeleton Inc.) for 2 hours at 4°C. Pelleted beads were washed three times with IP buffer. Protein bound to the beads was eluted with 1× Laemmli's buffer and subjected to 12% SDS–polyacrylamide gel electrophoresis (SDS-PAGE). Rho1 was detected with a monoclonal antibody recognizing HA (Covance).

Supplementary Material

Refer to Web version on PubMed Central for supplementary material.

Acknowledgments

We thank E. L. Weiss and D. J. Stillman for plasmids, strains, and critical reading of the manuscript. We are grateful to J. H. Grose for reagents and helpful discussions. We thank the Rutter lab for helpful discussions and J. Jaimez and A. Quint for technical support.

Funding: C.M.C. was supported as a predoctoral trainee by NIH Genetics Training Grant T32-GM07464. This work was supported by NIH grant RO1DK071962 (J.R.).

REFERENCES AND NOTES

1. Hardie DG. AMP-activated/SNF1 protein kinases: Conserved guardians of cellular energy. Nat Rev Mol Cell Biol. 2007; 8:774–785. [PubMed: 17712357]
2. Sengupta S, Peterson TR, Sabatini DM. Regulation of the mTOR complex 1 pathway by nutrients, growth factors, and stress. Mol Cell. 2010; 40:310–322. [PubMed: 20965424]
3. Zoncu R, Efeyan A, Sabatini DM. mTOR: From growth signal integration to cancer, diabetes and ageing. Nat Rev Mol Cell Biol. 2011; 12:21–35. [PubMed: 21157483]
4. Hardie DG. AMPK and Raptor: Matching cell growth to energy supply. Mol Cell. 2008; 30:263–265. [PubMed: 18471972]
5. Wullschleger S, Loewith R, Hall MN. TOR signaling in growth and metabolism. Cell. 2006; 124:471–484. [PubMed: 16469695]
6. Helliwell SB, Howald I, Barbet N, Hall MN. TOR2 is part of two related signaling pathways coordinating cell growth in *Saccharomyces cerevisiae*. Genetics. 1998; 148:99–112. [PubMed: 9475724]
7. Loewith R, Jacinto E, Wullschleger S, Lorberg A, Crespo JL, Bonenfant D, Oppliger W, Jenoe P, Hall MN. Two TOR complexes, only one of which is rapamycin sensitive, have distinct roles in cell growth control. Mol Cell. 2002; 10:457–468. [PubMed: 12408816]
8. Helliwell SB, Wagner P, Kunz J, Deuter-Reinhard M, Henriquez R, Hall MN. TOR1 and TOR2 are structurally and functionally similar but not identical phosphatidylinositol kinase homologues in yeast. Mol Biol Cell. 1994; 5:105–118. [PubMed: 8186460]
9. Kunz J, Henriquez R, Schneider U, Deuter-Reinhard M, Movva NR, Hall MN. Target of rapamycin in yeast, TOR2, is an essential phosphatidylinositol kinase homolog required for G_1 progression. Cell. 1993; 73:585–596. [PubMed: 8387896]
10. Schmidt A, Kunz J, Hall MN. TOR2 is required for organization of the actin cytoskeleton in yeast. Proc Natl Acad Sci USA. 1996; 93:13780–13785. [PubMed: 8943012]
11. Wullschleger S, Loewith R, Oppliger W, Hall MN. Molecular organization of target of rapamycin complex 2. J Biol Chem. 2005; 280:30697–30704. [PubMed: 16002396]
12. Schmidt A, Bickle M, Beck T, Hall MN. The yeast phosphatidylinositol kinase homolog TOR2 activates RHO1 and RHO2 via the exchange factor ROM2. Cell. 1997; 88:531–542. [PubMed: 9038344]
13. Nonaka H, Tanaka K, Hirano H, Fujiwara T, Kohno H, Umikawa M, Mino A, Takai Y. A downstream target of RHO1 small GTP-binding protein is PKC1, a homolog of protein kinase C, which leads to activation of the MAP kinase cascade in *Saccharomyces cerevisiae*. EMBO J. 1995; 14:5931–5938. [PubMed: 8846785]

14. Kamada Y, Qadota H, Python CP, Anraku Y, Ohya Y, Levin DE. Activation of yeast protein kinase C by Rho1 GTPase. J Biol Chem. 1996; 271:9193–9196. [PubMed: 8621575]
15. Qadota H, Python CP, Inoue SB, Arisawa M, Anraku Y, Zheng Y, Watanabe T, Levin DE, Ohya Y. Identification of yeast Rho1p GTPase as a regulatory subunit of 1,3-β-glucan synthase. Science. 1996; 272:279–281. [PubMed: 8602515]
16. Kohno H, Tanaka K, Mino A, Umikawa M, Imamura H, Fujiwara T, Fujita Y, Hotta K, Qadota H, Watanabe T, Ohya Y, Takai Y. Bni1p implicated in cytoskeletal control is a putative target of Rho1p small GTP binding protein in *Saccharomyces cerevisiae*. EMBO J. 1996; 15:6060–6068. [PubMed: 8947028]
17. Bickle M, Delley PA, Schmidt A, Hall MN. Cell wall integrity modulates RHO1 activity via the exchange factor ROM2. EMBO J. 1998; 17:2235–2245. [PubMed: 9545237]
18. Hao HX, Cardon CM, Swiatek W, Cooksey RC, Smith TL, Wilde J, Boudina S, Abel ED, McClain DA, Rutter J. PAS kinase is required for normal cellular energy balance. Proc Natl Acad Sci USA. 2007; 104:15466–15471. [PubMed: 17878307]
19. Rutter J, Probst BL, McKnight SL. Coordinate regulation of sugar flux and translation by PAS kinase. Cell. 2002; 111:17–28. [PubMed: 12372297]
20. Grose JH, Smith TL, Sabic H, Rutter J. Yeast PAS kinase coordinates glucose partitioning in response to metabolic and cell integrity signaling. EMBO J. 2007; 26:4824–4830. [PubMed: 17989693]
21. Smith TL, Rutter J. Regulation of glucose partitioning by PAS kinase and Ugp1 phosphorylation. Mol Cell. 2007; 26:491–499. [PubMed: 17531808]
22. Uesono Y, Toh-e A, Kikuchi Y. Ssd1p of *Saccharomyces cerevisiae* associates with RNA. J Biol Chem. 1997; 272:16103–16109. [PubMed: 9195905]
23. Chen CY, Rosamond J. *Candida albicans SSD1* can suppress multiple mutations in *Saccharomyces cerevisiae*. Microbiology. 1998; 144(Pt. 11):2941–2950. [PubMed: 9846729]
24. Jansen JM, Wanless AG, Seidel CW, Weiss EL. Cbk1 regulation of the RNA-binding protein Ssd1 integrates cell fate with translational control. Curr Biol. 2009; 19:2114–2120. [PubMed: 19962308]
25. Kaeberlein M, Andalis AA, Liszt GB, Fink GR, Guarente L. *Saccharomyces cerevisiae* SSD1-V confers longevity by a Sir2p-independent mechanism. Genetics. 2004; 166:1661–1672. [PubMed: 15126388]
26. Kaeberlein M, Guarente L. *Saccharomyces cerevisiae* MPT5 and SSD1 function in parallel pathways to promote cell wall integrity. Genetics. 2002; 160:83–95. [PubMed: 11805047]
27. Li L, Lu Y, Qin LX, Bar-Joseph Z, Werner-Washburne M, Breeden LL. Budding yeast SSD1-V regulates transcript levels of many longevity genes and extends chronological life span in purified quiescent cells. Mol Biol Cell. 2009; 20:3851–3864. [PubMed: 19570907]
28. Luukkonen BG, Séraphin B. A conditional U5 snRNA mutation affecting pre-mRNA splicing and nuclear pre-mRNA retention identifies SSD1/SRK1 as a general splicing mutant suppressor. Nucleic Acids Res. 1999; 27:3455–3465. [PubMed: 10446233]
29. Mir SS, Fiedler D, Cashikar AG. Ssd1 is required for thermotolerance and Hsp104-mediated protein disaggregation in *Saccharomyces cerevisiae*. Mol Cell Biol. 2009; 29:187–200. [PubMed: 18936161]
30. Moriya H, Isono K. Analysis of genetic interactions between DHH1, SSD1 and ELM1 indicates their involvement in cellular morphology determination in *Saccharomyces cerevisiae*. Yeast. 1999; 15:481–496. [PubMed: 10234786]
31. Tsuchiya E, Matsuzaki G, Kurano K, Fukuchi T, Tsukao A, Miyakawa T. The *Saccharomyces cerevisiae SSD1* gene is involved in the tolerance to high concentration of Ca^{2+} with the participation of *HST1/NRC1/BFR1*. Gene. 1996; 176:35–38. [PubMed: 8918228]
32. Uesono Y, Fujita A, Toh-e A, Kikuchi Y. The MCS1/SSD1/SRK1/SSL1 gene is involved in stable maintenance of the chromosome in yeast. Gene. 1994; 143:135–138. [PubMed: 8200529]
33. Kurischko C, Kim HK, Kuravi VK, Pratzka J, Luca FC. The yeast Cbk1 kinase regulates mRNA localization via the mRNA-binding protein Ssd1. J Cell Biol. 2011; 192:583–598. [PubMed: 21339329]

34. Kikani CK, Antonysamy SA, Bonanno JB, Romero R, Zhang FF, Russell M, Gheyi T, Iizuka M, Emtage S, Sauder JM, Turk BE, Burley SK, Rutter J. Structural bases of PAS domain-regulated kinase (PASK) activation in the absence of activation loop phosphorylation. J Biol Chem. 2010; 285:41034–41043. [PubMed: 20943661]
35. Daran JM, Dallies N, Thines-Sempoux D, Paquet V, Francois J. Genetic and biochemical characterization of the *UGP1* gene encoding the UDP-glucose pyrophosphorylase from *Saccharomyces cerevisiae*. Eur J Biochem. 1995; 233:520–530. [PubMed: 7588797]
36. Masuda CA, Xavier MA, Mattos KA, Galina A, Montero-Lomeli M. Phosphoglucomutase is an in vivo lithium target in yeast. J Biol Chem. 2001; 276:37794–37801. [PubMed: 11500487]
37. Helliwell SB, Schmidt A, Ohya Y, Hall MN. The Rho1 effector Pkc1, but not Bni1, mediates signalling from Tor2 to the actin cytoskeleton. Curr Biol. 1998; 8:1211–1214. [PubMed: 9811607]
38. Ozaki K, Tanaka K, Imamura H, Hihara T, Kameyama T, Nonaka H, Hirano H, Matsuura Y, Takai Y. Rom1p and Rom2p are GDP/GTP exchange proteins (GEPs) for the Rho1p small GTP binding protein in *Saccharomyces cerevisiae*. EMBO J. 1996; 15:2196–2207. [PubMed: 8641285]
39. Schmelzle T, Helliwell SB, Hall MN. Yeast protein kinases and the RHO1 exchange factor TUS1 are novel components of the cell integrity pathway in yeast. Mol Cell Biol. 2002; 22:1329–1339. [PubMed: 11839800]
40. Kimura K, Tsuji T, Takada Y, Miki T, Narumiya S. Accumulation of GTP-bound RhoA during cytokinesis and a critical role of ECT2 in this accumulation. J Biol Chem. 2000; 275:17233–17236. [PubMed: 10837491]
41. Kono K, Nogami S, Abe M, Nishizawa M, Morishita S, Pellman D, Ohya Y. G1/S cyclin-dependent kinase regulates small GTPase Rho1p through phosphorylation of RhoGEF Tus1p in *Saccharomyces cerevisiae*. Mol Biol Cell. 2008; 19:1763–1771. [PubMed: 18256282]
42. Alberts AS, Bouquin N, Johnston LH, Treisman R. Analysis of RhoA-binding proteins reveals an interaction domain conserved in heterotrimeric G protein β subunits and the yeast response regulator protein Skn7. J Biol Chem. 1998; 273:8616–8622. [PubMed: 9535835]
43. Yamochi W, Tanaka K, Nonaka H, Maeda A, Musha T, Takai Y. Growth site localization of Rho1 small GTP-binding protein and its involvement in bud formation in *Saccharomyces cerevisiae*. J Cell Biol. 1994; 125:1077–1093. [PubMed: 8195291]
44. Pende M, Kozma SC, Jaquet M, Oorschot V, Burcelin R, Le Marchand-Brustel Y, Klumperman J, Thorens B, Thomas G. Hypoinsulinaemia, glucose intolerance and diminished β-cell size in S6K1-deficient mice. Nature. 2000; 408:994–997. [PubMed: 11140689]
45. Longtine MS, McKenzie A III, Demarini DJ, Shah NG, Wach A, Brachat A, Philippsen P, Pringle JR. Additional modules for versatile and economical PCR-based gene deletion and modification in *Saccharomyces cerevisiae*. Yeast. 1998; 14:953–961. [PubMed: 9717241]

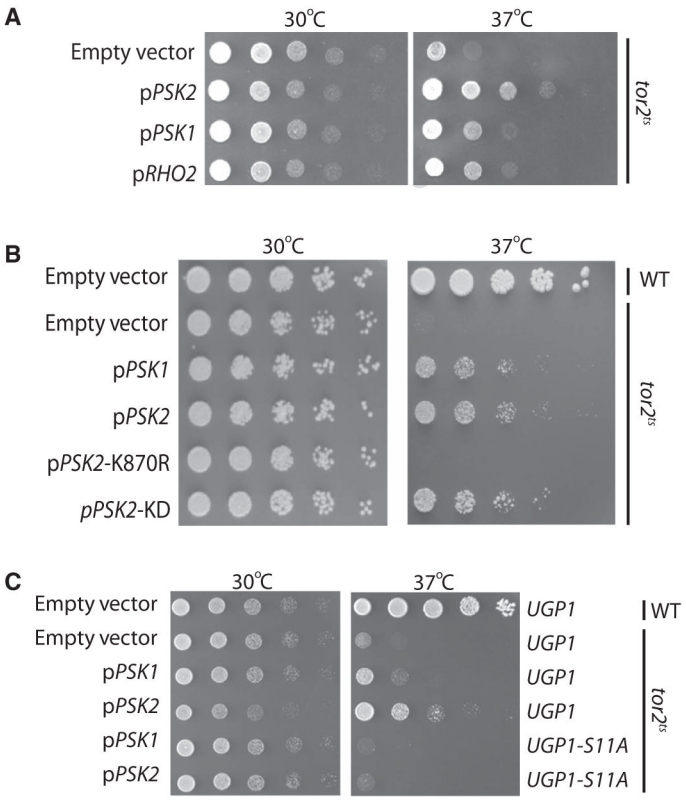

Fig. 1.

yPASK-dependent suppression of the *tor2*^{ts} growth phenotype requires kinase activity and Ugp1 phosphorylation. Strains of the indicated genotype were grown to saturation and serially diluted in water and spotted onto synthetic minimal medium lacking uracil. (**A**) Plasmids that contain all or part of *RHO2* (full length, three copies), *PSK1* (fragments recovered encoded amino acids 25 to 1356, 350 to 1356, and 10 to 1356), and *PSK2* (fragments recovered encoded amino acids 35 to 1101, 304 to 1101) were recovered from a high-copy suppressor screen of the *tor2*^{ts}. (**B**) High-copy plasmids that contain full-length *PSK1*, *PSK2*, *PSK2* kinase dead (K870R), or *PSK2* kinase domain only (*PSK2*-KD) were expressed from their endogenous promoters and assayed for an ability to suppress the growth defect of *tor2*^{ts}. WT, wild type. (**C**) High-copy plasmids that contain full-length either *PSK1* or *PSK2* were expressed in the presence of WT UGP1 or strains with *UGP1-S11A*. Experiments shown are representative of six independent experiments.

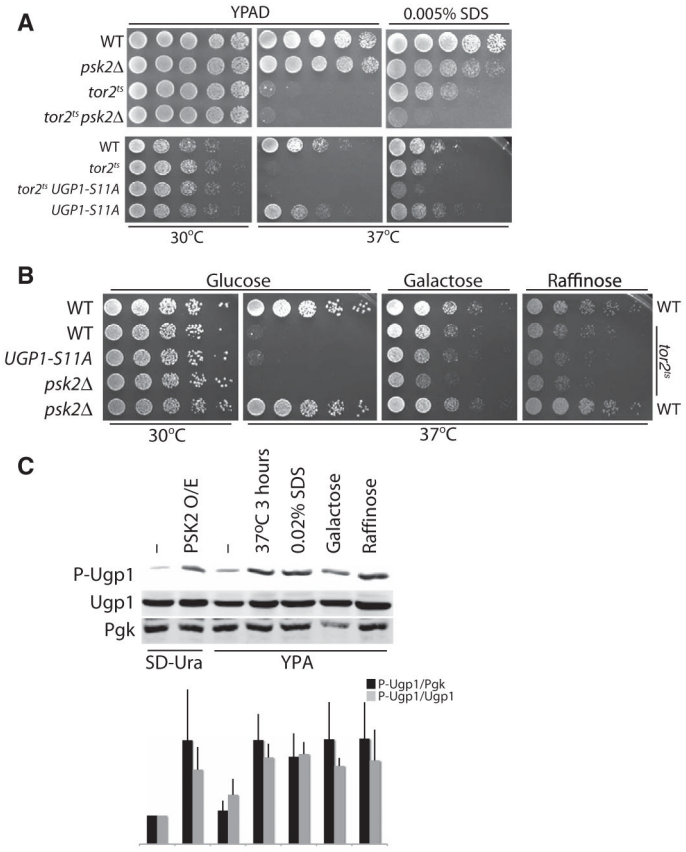

Fig. 2.

Activation of yPASK by either SDS or nonfermentative carbon sources suppresses the growth defect of *tor2*^{ts}. (**A**) Strains were grown to saturation and then serially diluted onto YPAD medium supplemented with 0.005% SDS. Experiments shown are representative of four independent experiments. (**B**) Strains were grown to saturation and then serially diluted on the indicated carbon source. Experiments are representative of four independent experiments. (**C**) WT strain was grown to saturation and then diluted to an optical density at 600 nm (OD_{600}) of ~0.2 in the synthetic medium lacking uracil (SD-Ura). Cells exposed to SDS or heat shock treatment for 3 hours were grown in YPAD medium. *PSK2* overexpression (PSK2 O/E) culture was grown in SD-Ura and was incubated at 37°C for 3 hours before harvest. Galactose and raffinose cultures were grown to saturation in SD-Ura medium and then diluted to an OD_{600} of ~0.2 in either SGal-Ura or SRaff-Ura. The graph shows the average and SD of four independent samples quantified with the LI-COR Odyssey Imaging software. Phosphorylated Ugp1 is shown as the ratio of total Ugp1 or the ratio of Pgk, which served as a loading control.

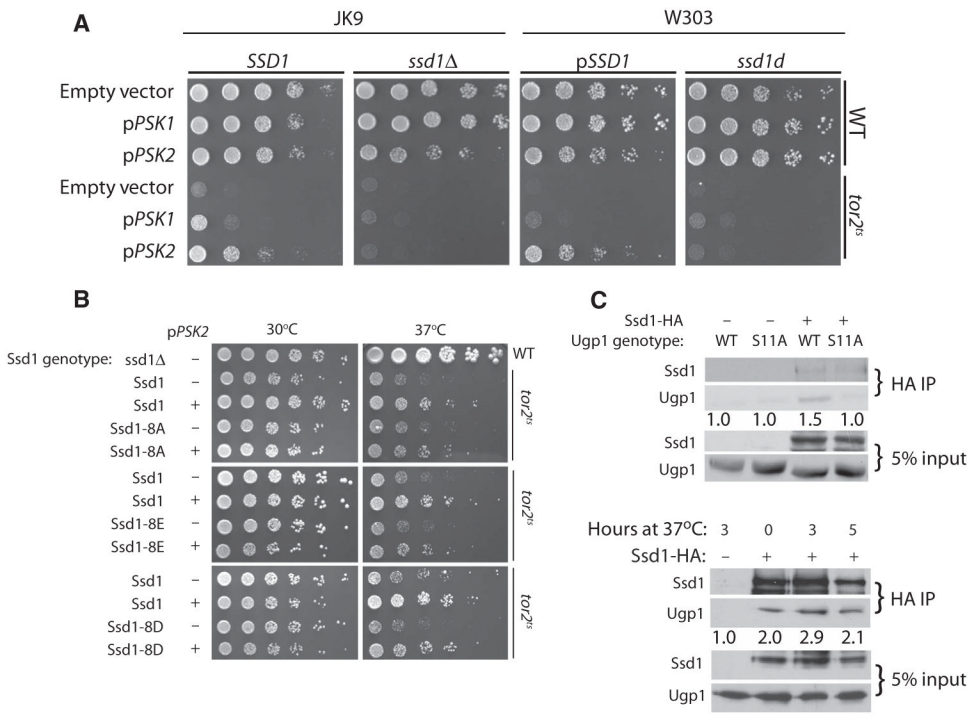

Fig. 3.

SSD1 is required for yPASK to suppress the growth defect of *tor2*^{ts}. (**A**) Expression of the wild-type *SSD1* in the W303 strain from its endogenous promoter on a CEN plasmid enabled *PSK2*-mediated suppression of the *tor2*^{ts} growth phenotype. Strains were grown at 37°C for 3 days. Experiments shown are representative of four independent experiments. (**B**) yPASK-dependent suppression of the *tor2*^{ts} growth phenotype occurred in the presence of nonphosphorylatable (Ssd1-8A) or phosphomimetic (Ssd1-8D, Ssd1-8E) Ssd1. Ssd1-8A, Ssd1-8D, or Ssd1-8E was expressed from a 2-μm plasmid with a minimal *CYC1* promoter. Strains were grown at the indicated temperature for 3 days. Experiments shown are representative of four independent experiments. (**C**) Ssd1 associates with Ugp1 in a phosphorylation-dependent manner with a peak of association at 3 hours of heat shock. The *tor2*^{ts} strain expressing Ssd1-HA was grown to log phase on synthetic glucose medium lacking uracil. Strains were heat-shocked at 37°C for 3 hours for the samples shown in the top blot and for the indicated times in those shown in the bottom. Ssd1 was detected with an antibody recognizing HA, and Ugp1 was detected with an antibody to endogenous Ugp1 (*n* = 5). This blot is quantified below and is representative of five independent experiments.

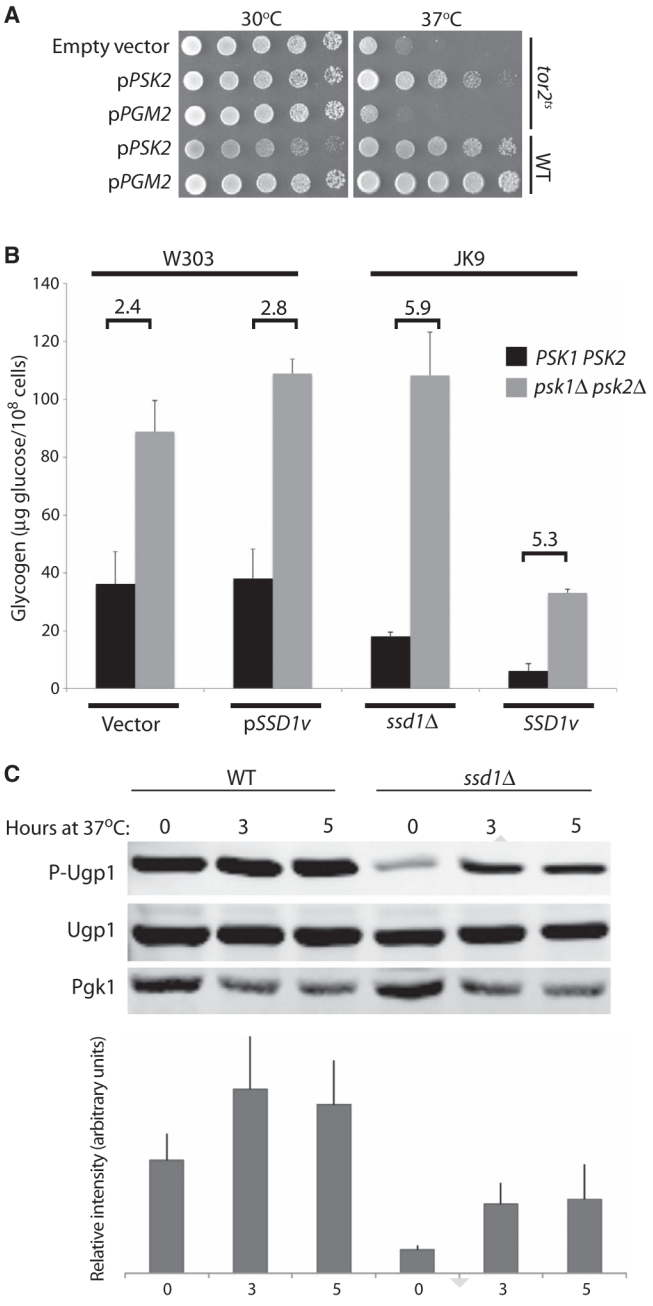

Fig. 4.

The metabolic function of Ugp1 is separable from its signaling role. (**A**) *PGM2* overexpression, which increases Ugp1 substrate availability, does not suppress the *tor2*^{ts} growth phenotype. Strains were grown at the indicated temperature for 2 days. Experiments shown are representative of four. (**B**) Fold change between *PSK1 PSK2* (WT) and *psk1*Δ *psk2*Δ for each *SSD1*genotype is indicated above bars. Indicated strains were grown at 30°C to an OD_{600} of ~1.0, harvested by centrifugation, and assayed for glycogen content. Data are presented as the average and SD of three samples. (**C**) Deletion of *SSD1* from the JK9 strain results in a decrease in Ugp1 phosphorylation. Quantification of four individual experiments (average and SD) is represented on the bar graph below a representative blot. Quantification

was performed with LI-COR Odyssey Imaging software. P-Ugp1 signal was normalized to total Ugp1. Strains were grown at 30°C and then shifted for the indicated time to 37°C.

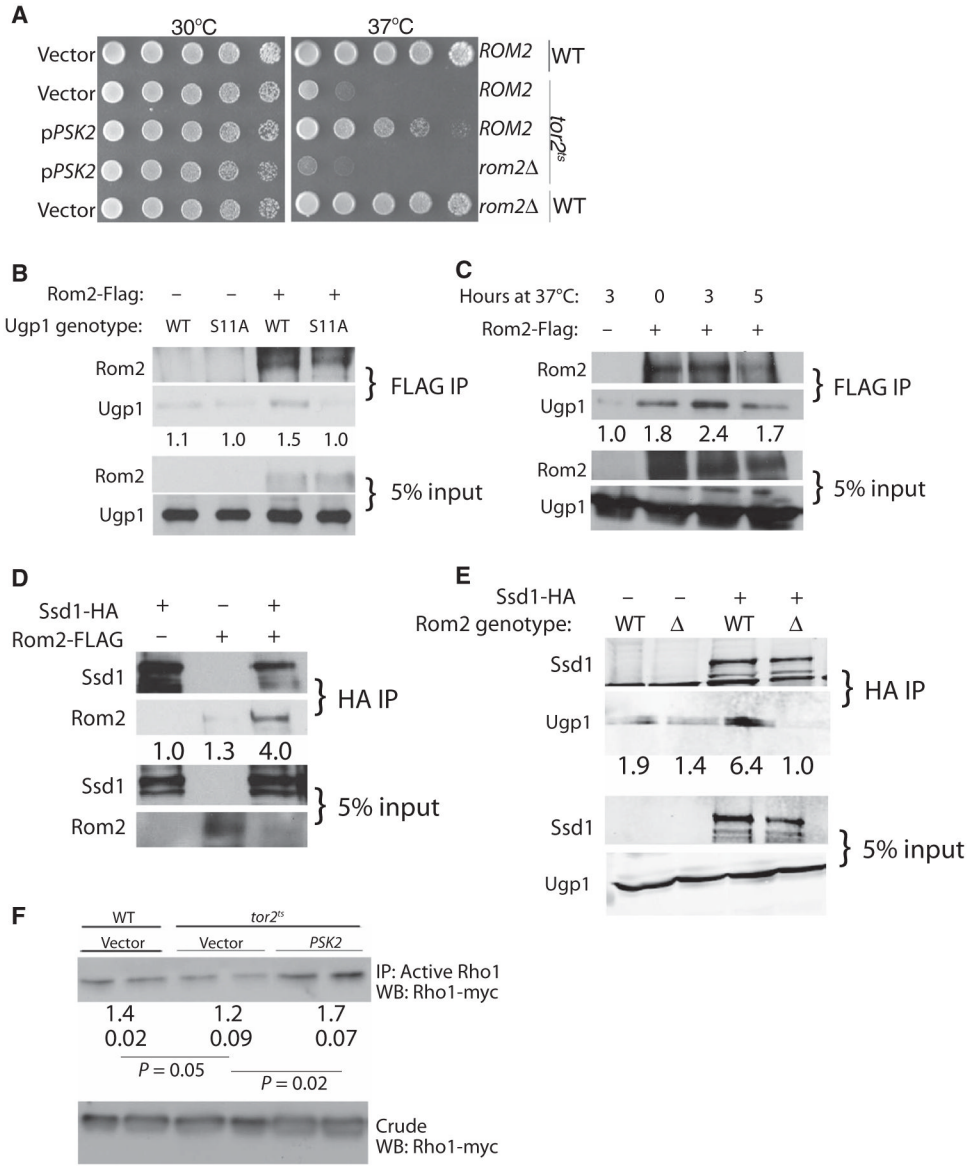

Fig. 5.

Rom2 is required for yPASK-dependent suppression of the *tor2*^{ts} growth phenotype and forms a complex with Ugp1. (**A**) Rom2 is necessary for *PSK2* overexpression to suppress the *tor2*^{ts}. Strains were grown at the indicated temperature for 2 days. (**B**) Rom2 interacts with Ugp1 in a phosphorylation-dependent manner. Numbers below the Ugp1 blot indicate quantification of bands by means of ImageJ with the amount of Ugp1-S11A in the control sample set to 1. Strains containing Rom2-FLAG at the endogenous locus with or without the Ugp1-S11A allele were grown to log phase and then subjected to immunoprecipitation with an antibody recognizing FLAG. Data are representative of four experiments. (**C**) Heat shock transiently increases the interaction between Rom2 and Ugp1. Immunoprecipitations were performed on a Rom2-FLAG strain with anti-FLAG beads and blotted for Ugp1. Data are representative of four experiments. Numbers below the Ugp1 blot indicate quantification of bands by ImageJ with the amount of Ugp1 in the control sample set to 1. (**D**) Rom2 and Ssd1 coimmunoprecipitate. Data are representative of three experiments. Numbers below the Rom2 blot indicate quantification of bands by ImageJ with the amount of Rom2 in the

absence of Rom2-FLAG set to 1. (**E**) Coimmunoprecipitation of Ssd1 and Ugp1 is absent in a *rom2*Δ strain. Strains were grown to mid-log phase and crude cell lysates were subjected to immunoprecipitation. Data are representative of three experiments. Numbers below the Ugp1 blot indicate quantification of bands by ImageJ with the amount of Ugp1 in the Ssd1-HA *rom2*Δ sample set to 1. (**F**) Rho1 activity is increased in cells overexpressing *PSK2*. Strains were grown to mid-log phase and GTP-bound Rho1 was immunoprecipitated with RBD beads ($n = 3$). Biological replicates were loaded in adjacent lanes and bands were quantified with ImageJ. Data are presented as the average and SD with *P* values determined by Student's *t* test.